

# Quasi Static Remanence in Weak Ferromagnets : Connection with Piezomagnetism

Namrata Pattnayak,<sup>1</sup> Arpan Bhattacharyya,<sup>2</sup> A. K. Nigam,<sup>3</sup> Sang-Wook Cheong,<sup>4</sup> and Ashna Bajpai<sup>1,5</sup>

<sup>1</sup>*Department of Physics, Indian Institute of Science Education and Research, Dr. Homi Bhabha Road, Pune 411008, India*

<sup>2</sup>*Saha Institute of Nuclear Physics, 1/AF Bidhannagar, Kolkata, India*

<sup>3</sup>*Department of Condensed Matter Physics and Material Science,*

*Tata Institute of Fundamental Research, Dr. Homi Bhabha Road, Mumbai 400 005, India*

<sup>4</sup>*Rutgers Center for Emergent Materials and Department of Physics and Astronomy,  
Rutgers University, Piscataway, New Jersey 08854, USA*

<sup>5</sup>*Center for Energy Science, Indian Institute of Science Education and Research, Dr. Homi Bhabha Road, Pune 411008, India\**

(Dated: March 28, 2017)

We explore remanence ( $\mu$ ) as a function of time and temperature, in a variety of rhombohedral antiferromagnets (AFM) which are also weak ferromagnets (WFM) and piezomagnets (PzM). These measurements, across samples with length scales ranging from nano to bulk, firmly establish the presence of a remanence that is quasi static in nature and exhibits a counter-intuitive magnetic field dependence. These observations unravel an ultra-slow magnetization relaxation phenomenon related to this quasi static  $\mu$ . This feature is also observed in a defect free single crystal of  $\alpha$ -Fe<sub>2</sub>O<sub>3</sub>, which is a canonical WFM and PzM. Notably,  $\alpha$ -Fe<sub>2</sub>O<sub>3</sub> is not a typical geometrically frustrated AFM and in single crystal form, it is also devoid of any size or interface effect, which are the usual suspects for a slow magnetization relaxation phenomenon. The underlying pinning mechanism appears exclusive to those AFM which are either symmetry allowed WFM, driven by Dzyaloshinskii-Moriya Interaction (DMI) or can generate this trait by tuning of size and interface. The qualitative features of the quasi static  $\mu$  indicate that such WFM are potential piezomagnets, in which magnetization can be tuned by *stress* alone.

## I. INTRODUCTION

Phenomenon of weak ferromagnetism in certain antiferromagnets, including the classic case of  $\alpha$ -Fe<sub>2</sub>O<sub>3</sub>, is associated with the experimental observation of a ferromagnetic (FM) like, spontaneous moment. This feature was initially attributed to a FM impurity phase in an otherwise AFM lattice; such as Fe<sub>3</sub>O<sub>4</sub> impurity in  $\alpha$ -Fe<sub>2</sub>O<sub>3</sub>.<sup>1-4</sup> This controversy was firmly resolved by Dzyaloshinskii in 1958,<sup>1</sup> who proposed a spin canting mechanism that leads to a weak FM like state and Moriya<sup>4</sup> who discovered the microscopic origin of this spin canting and its connection with spin orbit coupling (SOC). This is the celebrated Dzyaloshinskii-Moriya Interaction (DMI) which is now central to both fundamental and application based trends in contemporary condensed matter physics. Apart from exotic inhomogeneous spin textures and non collinear spin systems such as skyrmions, topological insulators and superconductors, DMI/SOC also brings into fore the role of antiferromagnet insulators in spintronics.<sup>5-14</sup>

In many of the symmetry allowed weak ferromagnets, which include rhombohedral AFMs like  $\alpha$ -Fe<sub>2</sub>O<sub>3</sub>, MnCO<sub>3</sub> and rutile AFMs like NiF<sub>2</sub> or CoF<sub>2</sub>, the phenomenon of stress induced moments or piezomagnetism, of the type ( $M_i = P_{ijk}\sigma_{jk}$ ) where  $\sigma$  is stress, was also predicted by Dzyaloshinskii.<sup>1</sup> Experimental observations of such stress induced moments were made by Borovik-Romanov in a variety of WFM/PzM single crystals in the seminal work spanning 1960-70.<sup>15-18</sup> On the similar lines of magnetoelectricity, wherein a magnetic moment can be created by *electric field* alone - for which Cr<sub>2</sub>O<sub>3</sub> is a prototype<sup>19,20</sup> - magnetic moment from *stress* alone can occur in PzM, for which  $\alpha$ -Fe<sub>2</sub>O<sub>3</sub> is a prototype.<sup>19,21,22</sup> It is also interesting that both Cr<sub>2</sub>O<sub>3</sub> and  $\alpha$ -Fe<sub>2</sub>O<sub>3</sub> are isostructural AFM but the piezomagnetic moments are observed in  $\alpha$ -Fe<sub>2</sub>O<sub>3</sub>, not in bulk Cr<sub>2</sub>O<sub>3</sub>. A picture

also emerged with a plausible explanation on the microscopic mechanism of PzM in these systems.<sup>23,24</sup>

In some of these WFM/PzM compounds or in their doped version,<sup>25</sup> an unusually slow magnetization relaxation was tracked through the measurement of remanence. This was further seen in ultra-thin films of Cr<sub>2</sub>O<sub>3</sub>,<sup>26</sup> in FM/AFM core shell systems where Cr<sub>2</sub>O<sub>3</sub> appeared as an ultra-thin surface layer<sup>27</sup> and also when Cr<sub>2</sub>O<sub>3</sub> is encapsulated inside carbon nanotubes<sup>28</sup> (CNT). These reports pointed towards some features in remanence which appear to be common, especially for AFM with the possibility of WFM/PzM. Most intriguing among these is ultra slow magnetization relaxation phenomenon, resulting in the observation of a quasi static remanence with a counter-intuitive field dependence.<sup>27,28</sup>

Interestingly, Cr<sub>2</sub>O<sub>3</sub> is not a symmetry allowed WFM/PzM but exhibits quasi static remanence only when it is in ultra-thin form. It is therefore important to systematically explore whether these features intrinsically exist in symmetry allowed WFM and to investigate the circumstances in which this can appear in systems with altered symmetry conditions, especially due to size/interface effects. In addition, what still remains an open question is whether piezomagnetism will always co-exist in all WFM and if so, what are the foot prints of this phenomenon? It is also important to explore possible means to isolate this subtle effect from routine magnetization measurements, wherein all other field dependent process contribute for any AFM (canted or otherwise) under magnetic field.

In this work we explore remanence in two rhombohedral AFM that are symmetry allowed WFM and PzM. This includes  $\alpha$ -Fe<sub>2</sub>O<sub>3</sub> with Neel transition temperature ( $T_N$ )  $\sim$  950 K and MnCO<sub>3</sub> with  $T_N \sim$  30 K. Here  $\alpha$ -Fe<sub>2</sub>O<sub>3</sub> is known to be a pure AFM upto 260 K and a WFM in the temperature range of 260-950 K.<sup>1,16</sup> The temperature at which  $\alpha$ -Fe<sub>2</sub>O<sub>3</sub>

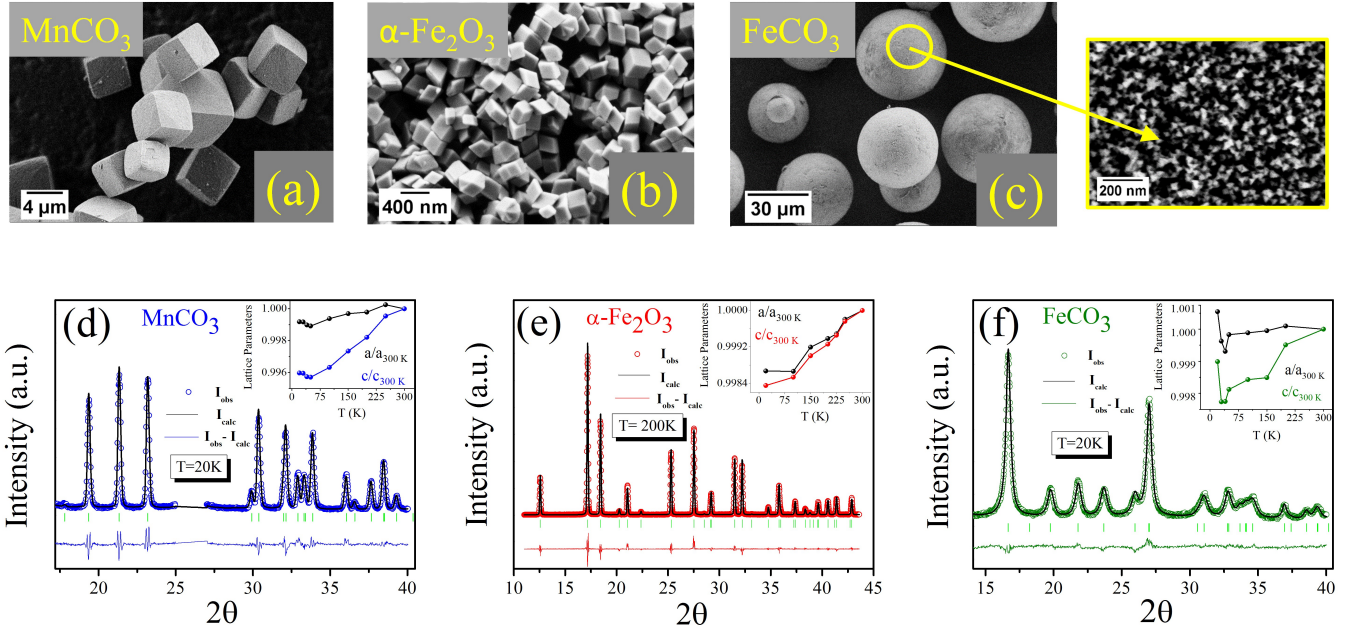


Figure 1. SEM images of (a) micro-cubes  $\text{MnCO}_3$  and (b) nano-cubes  $\alpha\text{-Fe}_2\text{O}_3$ . (c) SEM image of  $\text{FeCO}_3$  spheres with diameter  $\sim 20 \mu\text{m}$ . Each sphere consists of triangular  $\text{FeCO}_3$  nano particles  $\sim 5\text{-}10 \text{ nm}$ . (e)-(f) Synchrotron XRD data of  $\text{MnCO}_3$   $\alpha\text{-Fe}_2\text{O}_3$  and  $\text{FeCO}_3$  along with Rietveld fitting. The inset shows best fit lattice parameters derived from Rietveld profile refinement of  $I$  vs  $2\theta$  data recorded at different temperatures.

becomes WFM is also known as Morin Transition,  $T_M$  ( $\sim 260 \text{ K}$ ). It is advantageous to have a WFM near the room temperature. However the effect is known to be much weaker than  $\text{MnCO}_3$ .<sup>1</sup> We also investigate isostructural compound  $\text{FeCO}_3$  with  $T_N \sim 50 \text{ K}$ , for which there are conflicting reports in literature about the existence of WFM and PzM.<sup>1-3,17</sup> For such cases, size effects may play a prominent role as DMI can be dominant and enhanced at surfaces and interfaces.<sup>29</sup>

We study all three samples in the form of nano and mesoscopic crystals / particles and show a correlation between the structural parameter and the magnitude of pinned moment related to the quasi static remanence. In case of  $\alpha\text{-Fe}_2\text{O}_3$ , which is also a prototypical PzM near the room temperature, we confirm the ultra slow magnetization relaxation in its single crystal form, thus bringing out that the quasi static remanence is intrinsic. We also show that this feature can be substantially tuned by size effects, by comparing the magnitude of quasi static remanence in the single crystal and nano cubes of  $\alpha\text{-Fe}_2\text{O}_3$ .

## II. EXPERIMENTAL TECHNIQUES

Our primary tool here is DC magnetization in remanent state.<sup>30-36</sup> This enables us to track the magnetization relaxation (and hence pinning potential landscape) in all these WFM. The protocol of measuring remanence is as follows. The sample is cooled in the presence of a specified dc magnetic field  $H$  from above the  $T_N$  and magnetization  $M_{FC}$  is measured in Field Cooled (FC) cycle. At temperatures  $T \ll$

$T_N$  the magnetic field is switched off and the remanence ( $\mu$ ) is measured with  $H = 0$ . In this work, the remanence after a typical FC run is referred to as  $\mu_{FC}$  and can be measured either (i) as a function of increasing temperature or (ii) as a function of time at fixed  $T$ .

In case of  $\alpha\text{-Fe}_2\text{O}_3$ ,  $H$  is also applied from  $T \ll T_M$  and  $M_{ZFC}$  vs  $T$  is measured in warming cycle upto  $300 \text{ K}$ . The  $H$  is switched off at this temperature and the corresponding remanence,  $\mu_{ZFC}$  is recorded as a function of time ( $t$ ), while the temperature is held constant at  $300 \text{ K}$ .

Micro-cubes of  $\text{MnCO}_3$  (length  $\sim 2\text{-}4 \mu\text{m}$ ), nano-cubes of  $\alpha\text{-Fe}_2\text{O}_3$  (length  $\sim 200 \text{ nm}$ ) and polycrystalline spheres of  $\text{FeCO}_3$  (grain size  $\sim 5\text{-}10 \text{ nm}$ ) have been synthesized following the precipitation and hydrothermal routes<sup>37-39</sup> Fig. 1a-1c. The single crystal of  $\alpha\text{-Fe}_2\text{O}_3$  has been grown using Floating Zone technique. Scanning Electron Microscopy images are recorded using ZEISS ULTRA plus field-emission SEM. All the samples have been characterized using X-ray powder diffraction (XRD) using Bruker D8 advance with  $\text{Cu K}\alpha$  radiation ( $\lambda = 1.54056 \text{ \AA}$ ). (Supp. Info : Fig. S1-S3). Temperature variation of synchrotron XRD from  $20 \text{ K}$ - $300 \text{ K}$  has been conducted in BL-18 beam line, Photon Factory, Japan. The synchrotron XRD data has been fitted using Rietveld Profile Refinement. All three samples stabilize in rhombohedral structure and fitting has been done in hex setting. The XRD data along with the Rietveld fittings at few selected temperatures for each of the sample is shown in Fig. 1d-1f. The Temperature variation of refined lattice parameters  $a$  and  $c$  for the samples are shown in the respective insets in Fig. 1d-1f. The magnetization measurements have been carried out by using a

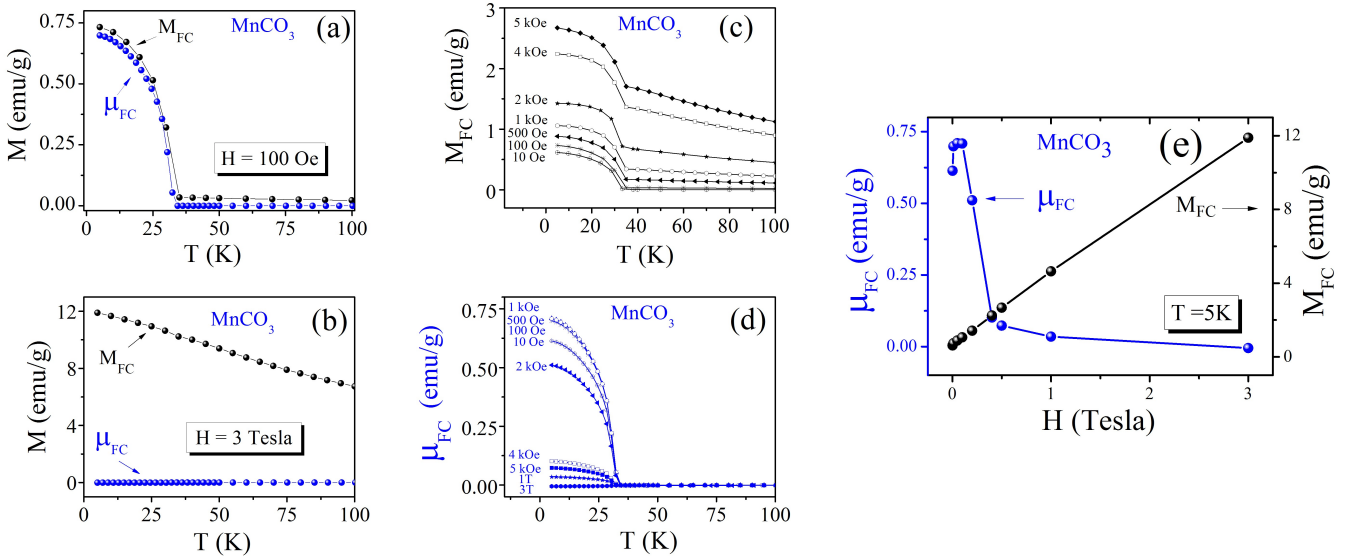


Figure 2. Black dots in (a) show magnetization measured while cooling ( $H = 100$  Oe) and blue dots are corresponding remanence ( $H=0$ ) measured while warming for MnCO<sub>3</sub> sample. (b) shows the same for  $H=3$  Tesla. (c)  $M_{FC}$  vs  $T$  at various  $H$  depicting regular AFM behavior with  $M_{FC}$  rising with rise in  $H$ . (d) shows corresponding  $\mu_{FC}$  vs  $T$  exhibit s strikingly different cooling  $H$  dependence. (e) compares the magnitude of  $M_{FC}$  (black dots, right axis) and  $\mu_{FC}$  (blue dots, left axis) at 5K as a function of (cooling)  $H$  for MnCO<sub>3</sub>.

superconducting quantum interference device (SQUID) magnetometer, Quantum Design MPMS-XL.

### III. RESULTS AND DISCUSSIONS

#### A. Remanence in MnCO<sub>3</sub>: Variation with $H$

Fig.2a shows  $M_{FC}$  vs  $T$ , (measured while cooling) in presence of  $H \sim 100$  Oe (black dots). The magnitude of  $M_{FC}$  at 5K  $\sim 0.75$  emu/g. After removal of  $H$  at 5K, a part of the magnetization decays instantaneously. However, a significant part of magnetization remains pinned, resulting in the observation of remanence. This remanence ( $\mu_{FC}$ ) shows almost no further decay as a function of time, as long as the temperature is held constant at 5K. As evident from Fig.2a, the magnitude of the  $\mu_{FC}$  at 5K is  $\sim 0.7$  emu/g for this run. On increasing the temperature,  $\mu_{FC}$  vs  $T$  (measured while warming) shows a variation which is qualitatively similar to  $M_{FC}$  vs  $T$  right up to the  $T_N$  as shown in Fig.2a (blue dots). In the paramagnetic tail, the  $\mu_{FC}$  vanishes, as is expected.

Fig.2b shows the same for  $H \sim 3$  Tesla, for which  $M_{FC} \sim 12$  emu/g whereas the  $\mu_{FC} \sim 10^{-5}$  emu/g at 5 K. Thus the  $\mu_{FC}$  is vanishingly small for 3 Tesla run. We would consider the  $\mu$  of this magnitude to be roughly arising from the quenched field of SQUID superconducting magnet, which may be  $\sim 5$ -10 Oe and can vary from run to run<sup>40</sup>. The data contained in Fig.2 clearly indicates that the magnitude of  $\mu$  is almost equivalent to that of  $M_{FC}$  for lower (cooling)  $H$  whereas it is negligible for very high  $H$ .

For all the intermediate magnetic fields, the  $M_{FC}$  vs  $T$  data are plotted in 2c and their corresponding  $\mu_{FC}$  vs  $T$  are plotted

in Fig.2d. As is evident from these data, the magnetization increases with increasing  $H$ , consistent with a regular AFM behaviour. However, the corresponding remanence varies with the strength of the magnetic field in an unexpected way. Here the remanence is first seen to rise with increasing  $H$ , upto a critical field. Thereafter it decreases with increase in field and eventually vanishes beyond another critical field.

To clearly bring out the unusual (cooling) field dependence of the  $\mu_{FC}$ , we compare the magnitude of both  $M$  and  $\mu$  at 5K. These data points are extracted from different  $M_{FC}$  vs  $T$  and their corresponding  $\mu_{FC}$  vs  $T$  runs Fig.2e. Here  $M_{FC}$  is seen to increase with increasing  $H$ , as is expected for a regular AFM, whereas the  $\mu_{FC}$  initially rises with increasing  $H$ , followed by a sharp drop. The  $\mu_{FC}$  completely vanishes at very high field. The type of field dependence of  $\mu$  is not expected for either a regular FM or AFM.<sup>31-33</sup>

#### B. Remanence in MnCO<sub>3</sub>: Variation with time

To check the stability of the remanence as a function of time, we also performed relaxation rate measurements. After a typical  $M_{FC}$  vs  $T$  and subsequent removal of  $H$ , we obtained  $\mu_{FC}$  vs time, while the temperature is held constant at 5K Fig.3. These remanence data, obtained for three different cooling fields, again bring forward two distinct magnetization relaxation rate, one of which is ultra-slow. We observe that for measurement times of about 3 hours, the  $\mu_{FC}$  shows no appreciable decay. Consistent with the data presented in Fig.2d, magnitude of the  $\mu_{FC}$  is seen to vary with cooling field  $H$  in a way, which is not obvious from the routine temperature  $M$ - $H$  isotherms. For the chosen cooling fields of 100 Oe, 1 kOe and 5 kOe, the  $\mu_{FC}$  values are  $\sim 93\%$ ,  $70\%$  and  $3\%$  of their



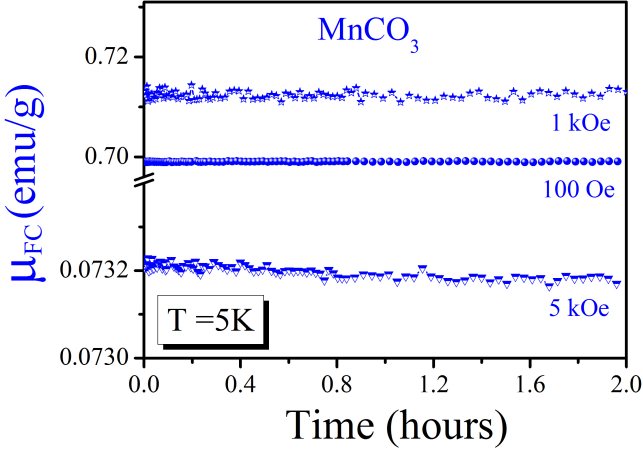


Figure 3. Remanence as a function of time for three different cooling fields at a fixed temperature of 5K for  $\text{MnCO}_3$ . These data show that the remanence is almost constant over a time period of 2 hours, thus depicting its quasi static nature.

corresponding  $M_{FC}$  values. Thus the data contained in Fig.3 confirms presence of the remanence that is quasi static in nature with ultra-slow magnetization dynamics, and exhibits a counter intuitive  $H$  dependence.

### C. Remanence and structural parameters in $\alpha\text{-Fe}_2\text{O}_3$ , $\text{FeCO}_3$ and $\text{MnCO}_3$

Similar measurements were also conducted for  $\alpha\text{-Fe}_2\text{O}_3$  and  $\text{FeCO}_3$  samples. Fig.4a compares  $\mu_{FC}$  vs  $H$  data at 5K (extracted from various  $\mu_{FC}$  vs  $T$  runs for each sample) for all three samples. For  $\text{MnCO}_3$ ,  $\mu_{FC}$  vs  $H$  rises and falls rather sharply with peak value at  $\sim 500$  Oe. Other two samples also exhibit a sharp rise, followed by a slight decline in  $\mu_{FC}$  above 1 Tesla, but the fall is not as rapid as what is seen for  $\text{MnCO}_3$ . Fig.4b compares  $\mu_{FC}$  vs time at the cooling field 1 kOe for all three samples. All samples exhibit a slow magnetization relaxation in  $\mu_{FC}$  vs time measurements. At 1 kOe, the magnitude of the remanence is atleast an order of magnitude higher for  $\text{MnCO}_3$  as compared to other two samples. In addition, the stability of the remanence as a function of time is also higher for this sample.

To correlate the observed features in  $\mu$  with structural parameters, the temperature variation of  $a$  and  $c$  lattice parameters is studied. As can be seen from the inset of Fig.1d, for  $\text{MnCO}_3$ , both  $a$  and  $c$  decrease with reducing temperature monotonically till about the  $T_N$ , however an expansion in both the lattice parameters is observed just below its AFM transition temperature. In addition, for  $\text{MnCO}_3$  the lattice parameter  $c$  is seen to fall much rapidly with reducing temperature as compared to  $a$  (inset of Fig.1d). On the contrary, for  $\alpha\text{-Fe}_2\text{O}_3$ , the pattern of temperature variation for  $c$  and  $a$  are quite similar in nature and a slight trend of expansion in both lattice parameters is observed around its WFM region (Fig.1e). For all

three samples, both lattice parameters exhibit a slight anomaly below  $T_N$  (or around WFM in case of  $\alpha\text{-Fe}_2\text{O}_3$ ), however the effect is more pronounced for the  $\text{MnCO}_3$ . Fig.4c compares normalized  $c/a$  ratio as a function of temperature for all three samples. This normalization is w.r.t  $c/a$  ratio at 300 K for each sample. We find that the  $c/a$  ratio shows a more rapid decline with reducing temperature and the effect is more pronounced for  $\text{MnCO}_3$ . This trend correlates with the stability and magnitude of the  $\mu$ , both of which are relatively higher for  $\text{MnCO}_3$ .

For physical mechanism related to the pinned moment that results in ultra-slow magnetization relaxation, a number of phenomena such as glassy phase, superparamagnetism, defect pinning in a regular FM or AFM, exchange bias at FM/AFM interface etc. can be considered. Such phenomena are known to result in slow relaxation with a variety of temporal functional forms.<sup>30–35</sup> However the mechanism behind the pinning seen in these samples appears to be different from above mentioned phenomena. For instance, considering size effects,  $\text{MnCO}_3$  shows most robust pinning at lower fields. However, the sample used for magnetization measurements consists of fairly big crystallites ( $\sim 2\text{-}4\ \mu\text{m}$ ) therefore it is less likely that the slow relaxation is arising from size reduction or nano scaling. It is neither a glassy system, nor a nano scale FM which can exhibit superparamagnetic traits. Crystallites are also regular shaped with well-formed facets and therefore it also cannot be classified as a regular AFM or FM with defect pinning playing a role. Also, for a regular AFM/FM, the  $\mu$  should have shown saturation<sup>31</sup> with  $H$ , rather than the sharp drop such as seen in Fig. 2e.

To understand the nature of pinning with the presence of WFM and to confirm if this effect is intrinsic, we also explored it in a single crystal (SC). For this purpose, we chose a SC of  $\alpha\text{-Fe}_2\text{O}_3$ . Among the samples considered here,  $\alpha\text{-Fe}_2\text{O}_3$  is known to be both pure AFM (upto 260 K) and WFM (260 K - 950 K). Thus  $\alpha\text{-Fe}_2\text{O}_3$  provides a unique opportunity to probe both AFM and WFM phase in the same sample, which individually exist in a wide temperature range.

### D. Remanence in a Single Crystal of $\alpha\text{-Fe}_2\text{O}_3$

Main panel of Fig.5a shows  $M_{FC}$  Vs  $T$  for a SC of  $\alpha\text{-Fe}_2\text{O}_3$  sample. The Morin transition at  $\sim 260$  K demarcates the two regions, pure AFM and WFM for this sample. From  $M_{FC}$  vs  $T$  at 1 kOe, along  $a$  axis, we note that magnitude of  $M_{FC}$  is roughly  $\sim 0.3$  emu/g in WFM region and  $\sim 0.01$  emu/g in the pure AFM region. After switching off the field at 5K, corresponding  $\mu_{FC}$  vs  $T$  in warming cycle is shown in the main panel of Fig.5b. The  $\mu_{FC}$  is found to be negligibly small ( $10^{-5}$  emu/g) in the pure AFM region and substantially large in WFM region ( $\sim 0.2$  emu/g).

Here, the sign of the  $\mu_{FC}$  is found to be negative w.r.t the direction of applied  $H$ . From a number of such  $\mu_{FC}$  vs  $T$  data along  $a$  axis, we find that the sign of  $\mu_{FC}$  at 300 K remains primarily negative and its magnitude shows a slight decrease with increasing magnetic field (inset in Fig.5b). Though the sign of the  $\mu_{FC}$  along  $a$  axis is not commensurate with the

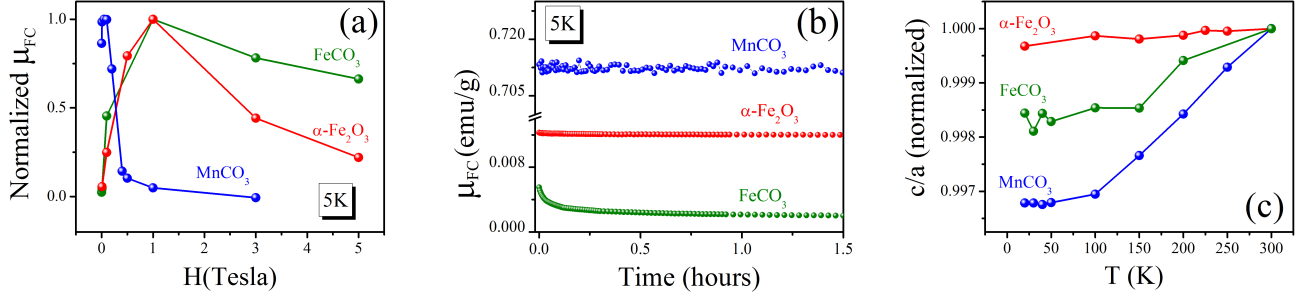


Figure 4. **(a)** Compares normalized  $\mu_{FC}$  as a function of (cooling)  $H$  for all three samples. **(b)** Compares  $\mu_{FC}$  as a function of time in all three samples. The observation of the quasi static nature of remanence is unambiguous in case of  $\text{MnCO}_3$  as well as  $\alpha\text{-Fe}_2\text{O}_3$ . **(c)** shows  $c/a$  ratio using refined lattice parameters obtained at various temperature from Rietveld fitting of synchrotron XRD data. The  $c/a$  ratio has been normalized with its value at 300 K.

direction applied  $H$  while cooling, its magnitude is substantial only in WFM region<sup>41</sup>.

For this sample, we performed  $\mu$  vs time measurements to check the stability of the pinned moments. We measured remanence in both FC and ZFC protocols across the Morin transition temperature of  $\alpha\text{-Fe}_2\text{O}_3$ . The  $\mu_{FC}$  and  $\mu_{ZFC}$ , both measured along  $c$  axis, are compared in Fig.5c. While  $\mu_{FC}$  in pure AFM region is  $\sim 10^{-5}$  emu/g (inset of Fig.5c), the  $\mu_{ZFC}$ , in WFM region is about  $\sim 0.05$  emu/g (main panel, Fig.5c). In this particular run,  $\mu_{ZFC}$  is positive and is commensurate with the direction of  $H$ . However, from a number of  $\mu_{ZFC}$  vs time cycles in positive  $H$ , we observe that the magnitude of  $\mu_{ZFC}$  again varies from 0.05-0.2 emu/g but its sign primarily remains negative. Such ambiguity with sign has also been observed in the sign of stress induced moments in some WFM/PzM on repeated cooling.<sup>15</sup> The reason for such ambiguity in case of remanence, (which does not appear in regular in-field magnetization) is also discussed in the later part of the text. However, from the SC remanence data, the presence of substantial  $\mu$  in WFM region is confirmed. We also note a slight variation (5%) in the magnitude of  $\mu$ , from run to run in the WFM region.

Interestingly, we also observe a slight trend of rise ( $\sim$  a few% of total remanence) in  $\mu_{ZFC}$  vs time data, as shown in Fig.5c. This data indicates that on application of  $H$ , moments continue to reorient slowly in WFM regime. On removal of  $H$ , their time relaxation is slow as well. This result prompted us to perform *waiting time* dependence, usually employed for glassy systems.<sup>34</sup> For *waiting time* runs,  $M_{ZFC}$  vs  $T$  was measured from below the Morin transition temperature in warming cycle. At 300 K the magnetic field was kept on for *waiting time* of either 1 minute or 100 minutes, prior to finally switching it off for the remanence measurements. These  $\mu_{ZFC}$  vs *time* data parallel to  $c$  axis plotted in the main panel of Fig.5d are for 1 min (red dots) or 100 min (black dots) waiting time respectively. The inset shows the same for  $\mu_{ZFC}$  parallel to  $a$  axis after 100 min of *waiting time*. These data further confirms that the system in WFM state has ultra-slow time response and memory effects.

$\alpha\text{-Fe}_2\text{O}_3$  is not a frustrated AFM and in the single crystal form, size/interface related phenomena cannot account for

the memory effects and ultra-slow magnetization dynamics. From the observation of quasi static remanence in single crystal, together with similar features observed in  $\text{MnCO}_3$ , we conclude that the ultra-slow magnetization dynamics can be taken as indicative of the presence of WFM. This ultra-slow dynamics also appears to be associated with the microscopic details of the AFM domain which turn WFM due to spin canting.

#### E. DMI driven Spin Canting and Ultra Slow Magnetization Dynamics

Considering the microscopic reason for the ultra-slow magnetization dynamics in these systems, we recall the details of magnetic structure in all these compounds. In the rhombohedral systems considered here, such as  $\alpha\text{-Fe}_2\text{O}_3$ , in pure AFM region, the spins are arranged along  $c$  axis whereas in the WFM region, the spins point in the basal plane, arranged in a specific sequence, which differs from pure AFM phase and the net FM moment due to the spin canting, is in the  $c$  direction.<sup>1</sup> This net FM moment in an otherwise AFM is responsible for WFM. This requires the specific magnetic point group symmetry as shown in reference 1. For the sake of clarity, the spin arrangement in pure AFM and WFM state is drawn in Fig.6a. The spin arrangement shown in the right side of Fig.6a is essential for the observation of WFM. This should also limit the possible ways in which an AFM domain can exist in the WFM region.

For a regular AFM, on the application of the  $H$ , the induced magnetization is driven by the Zeeman energy and the magnetocrystalline anisotropy. However, the addition factor in WFM will include response from canted spins, related to the anisotropic exchange as well. On removal of  $H$ , the reversal of the WFM domain will have to be accompanied by the reversal of the AFM moment which is energetically unfavorable.<sup>15</sup> Once a AFM domain with spin canting (associated with WFM) is formed, guided by a cooling  $H$  applied from above the AFM to PM transition, it is energetically unfavourable for these domains to relax, when the  $H$  is removed. This feature is only observed upto a critical value of  $H$ . Be-

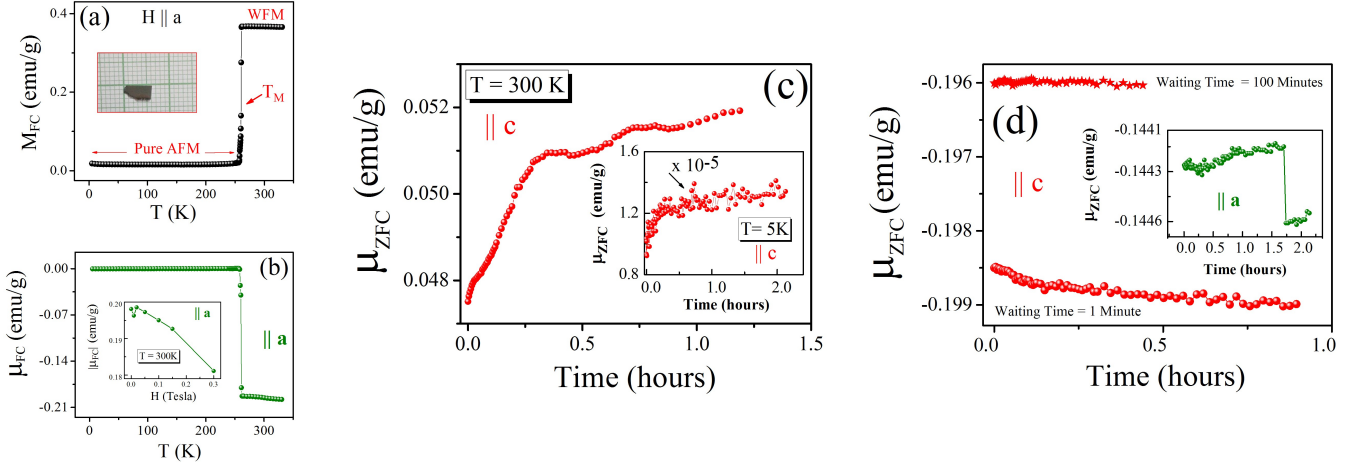


Figure 5. (a)  $M_{FC}$  vs  $T$  for a single crystal of  $\alpha$ -Fe<sub>2</sub>O<sub>3</sub>, with  $H$  (1kOe) parallel to  $a$  axis. The pure AFM and WFM regions are distinguished by  $T_M$ , the well-known Morin transition, marked as red arrow in the figure. The inset shows the picture of the  $\alpha$ -Fe<sub>2</sub>O<sub>3</sub> single crystal. (b) shows  $\mu_{FC}$  vs  $T$  run corresponding to the  $M_{FC}$  vs  $T$  run shown in (a). Here the remanence is vanishingly small in the pure AFM region and finite in the WFM region. The inset shows  $\mu_{ZFC}$  at 300 K along  $a$  axis as a function of various (cooling)  $H$ . These data points are extracted from various  $\mu_{FC}$  vs  $T$  runs. (c) shows  $\mu_{ZFC}$  vs time at 300 K (WFM region) measured along the  $c$  axis. The inset shows  $\mu_{FC}$  vs time along  $c$  axis at 5K (pure AFM region). While  $\mu_{FC}$  is negligibly small in the pure AFM region, it is substantially large (atleast by a few orders of magnitude) in the WFM region. (d) Main panel shows  $\mu_{ZFC}$  vs time measurements parallel to  $c$  axis for waiting time of 100 minutes (red stars) and 1 minute (red dots). Inset shows  $\mu_{ZFC}$  vs time parallel to  $a$  axis showing discrete jump.

yond this, the magnetization dynamics is driven by Zeeman and magnetocrystalline anisotropy. The magnetization relaxation in this case is much faster, similar to what is observed for a normal AFM under magnetic field. However, below this critical field strength, the WFM domain configuration is guided by the sign of  $H$  field, when, it is applied from  $T \gg T_N$ . This also explains the ambiguity with sign, as observed in case of  $\alpha$ -Fe<sub>2</sub>O<sub>3</sub>.

For further checking the ambiguity with sign, we also revert back to MnCO<sub>3</sub> which has a  $T_N \sim 30$  K and hence the  $H$  can be applied in the paramagnetic region for each FC cycle. Fig. 6b shows  $M_{FC}$  vs  $T$  data recorded while cooling from above  $T_N$ , down to 5 K, in presence of  $H = +100$  Oe. At 5K the  $H$  is switched off and the quasi static remanence is observed which has is positive in magnitude as the WFM domain configuration is already guided by the  $H = +100$  Oe. Temperature still held at 5K, we again apply  $H = -100$  Oe and subsequent to this, the  $M$  vs  $T$  is measured in warming cycle (FH cycle) in presence of  $H = -100$  Oe. As is evident from the data shown in Fig. 6b, once pinned in WFM state from above  $T_N$  by a positive  $H$ , the negative field cannot change the sign of pinned moment. The measured magnetization in heating cycle is basically due to the presence of positive remanence, stabilized during previous ( $H = +100$  Oe) FC cycle. This data explains the ambiguity related with the sign of remanence, especially when the  $H$  field is applied in WFM region. This ambiguity is the consequence of ultra slow magnetization relaxation associated with domain configuration in WFM region.

The robustness of the such pinned moments results in quasi static remanence at lower  $H$ . At higher  $H$ , the interplay is between Zeeman, exchange energy, as is usually observed for a

regular AFM. The ambiguity related with the sign of  $\mu$  in single crystal of  $\alpha$ -Fe<sub>2</sub>O<sub>3</sub> is related with configuration of AFM domains which cant due to DMI, even in the absence of  $H$ . On cooling or heating in presence of  $H$  leads to stabilization of these canted AFM domains in different configurations, compatible with the interplay of various energy scales involved. This feature again indicates that the net moment related to quasi static  $\mu$  is associated with net FM moment arising due to spin canting in otherwise AFM.

## F. Quasi Static Remanence and Piezomagnetism

A general consensus in the literature is PzM is connected with the transition from pure AFM to WFM state in an otherwise AFM and one of the mechanism that leads to the WFM state is associated with DMI.<sup>18</sup> More importantly, the direction of net FM moment in the WFM phase is seen to coincide with the direction of PzM.<sup>15</sup> This appears to be the case of rhombohedral WFM discussed here. The observation of quasi static remanence indicates presence of a very robust pinning mechanism. The remanence measurement also show that once the WFM domains have been formed, guided by the magnetic field from above the magnetic transition temperature, removal of the magnetic field does not make any difference. The moments are pinned due to DMI driven canting. It is also well known that magnetization reversal in piezomoments would require reversal of WFM sublattice which is energetically unfavorable.<sup>17</sup> This clearly connects the presence of DMI and quasi static remanence (and consequently the ultra slow magnetization dynamics). It is also to be recalled that memory effects and ambiguity with sign (which we ob-

serve in remanence  $\alpha$ -Fe<sub>2</sub>O<sub>3</sub> w.r.t the sign of the applied H) has also been observed in the sign of stress induced moments in WFM/PzM on repeated cooling.<sup>15,21</sup> The data presented in Fig.6b explains the ambiguity with the sign and the robustness of the pinned moments related to DMI driven canting and PzM. This also points towards the connection of WFM and Pzm and we can say that the WFM phase is intimately related with the onset of transverse PzM in rhombohedral AFM.

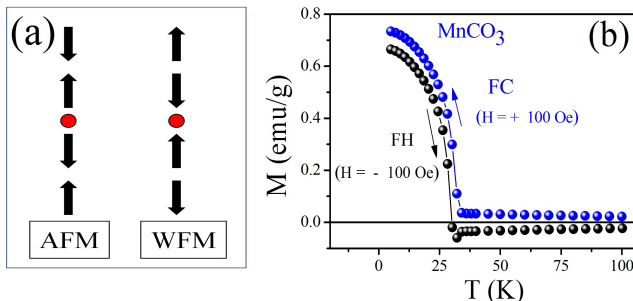


Figure 6. **(a)** shows the spin configuration in AFM (left) and WFM (right) state for rhombohedral AFM discussed here. The red dot is centre of inversion. **(b)** shows  $M$  Vs  $T$  recorded while cooling in presence of  $H = +100$  Oe (blue dots). At 5K, the  $H = +100$  Oe is removed and  $H = -100$  Oe is applied while the temperature is held constant at 5K. Subsequently  $M$  vs  $T$  in presence of  $H = -100$  Oe is again recorded in warming cycle (black dots). The measured magnetization is basically the remanence prepared during the previous cooling cycle. Since the sample is already in the WFM state, the presence of  $H = -100$  Oe is not sufficient to rotate the magnetization. The robustness of pinned moment, which leads to quasi static remanence, for  $\text{MnCO}_3$  is evident from this data.

From present data it appears that ultra-slow magnetization dynamics and associated pinning mechanism arises from the WFM and such systems are potential PzM. The magnitude of the WFM/PzM is further related to lattice parameters, especially  $c/a$  ratio in all these rhombohedral systems. A systematic study of such canonical WFM/PzM such as presented here, points towards the footprints of this phenomenon by simple magnetization measurements. It is to be emphasized that the system considered here are AFM with WFM trait. These are not frustrated AFM or a disordered glassy system / spin glass in conventional sense, which can exhibit slow relaxation for various other reasons. Therefore it is very interesting to observe ultra-slow relaxation in a completely ordered system in which these features are correlated with DMI/SOC.

From our data, it can be concluded that for micro-cubes of  $\text{MnCO}_3$  and nano-cubes and single crystal of  $\alpha\text{-Fe}_2\text{O}_3$ , the presence of ultra-slow magnetization dynamics is associated with intrinsic WFM. The temperature variation of remanence data on nano-cubes and single crystal of  $\alpha\text{-Fe}_2\text{O}_3$  especially

bring out that the quasi static remanence can be significantly tuned by nanoscaling, as also has been observed earlier.<sup>27,28</sup> For  $\text{FeCO}_3$ , data is not sufficient to conclude whether effects is intrinsic or it is arising from the size reduction, as the sample comprises of 5-10 nm particles of  $\text{FeCO}_3$ . In such cases, the strain in lattice parameters can also stabilize the WFM phase.<sup>26-28</sup> It is to be noted that is relatively hard to stabilize  $\text{FeCO}_3$  in the form of macroscopic crystallites for ruling out size effects. However, we are in the process of exploring systematic size effects in  $\text{FeCO}_3$ . We also assert that for systems which are isostructural AFM with  $\alpha\text{-Fe}_2\text{O}_3$ , such as  $\text{Cr}_2\text{O}_3$  (which is definitely not asymmetry allowed PzM) and  $\text{FeCO}_3$  (for which there are conflicting reports in the literature) the strain in the lattice parameter arising from size effects is likely to stabilize the WFM/PzM phase.<sup>27,28</sup>

## IV. CONCLUSION

In conclusion, we explore two rhombohedral antiferromagnets that are weak ferromagnets and observe an ultra-slow magnetization dynamics and associated with this, a very robust pinning mechanism which is intimately related to the weak ferromagnetism arising from spin canting. This spin canting is associated with DMI for the rhombohedral antiferromagnets discussed here. This feature is intrinsic in nature and the slow relaxation observed here does not relate with pinning arising from the glassy phase, magnetocrystalline anisotropy or routine exchange bias. The DMI in WFM phase is clearly connected with the possibility of stress induced moments or piezomagnetism. Finally, piezomagnetism, though not as widely explored or utilized, say as piezoelectricity, can have a variety of applications including those related to FM/AFM interfaces, in which the FM moment can be pinned by a PzM, and the effect should be tunable by stress alone.

## V. ACKNOWLEDGMENTS

Authors thank Sunil Nair (IISER Pune) for SQUID magnetization measurements. AB acknowledges Department of Science and Technology (DST), India for funding support through a Ramanujan Grant and the DST Nanomission Thematic Unit Program. SWC is funded by the Gordon and Betty Moore Foundations EPIQS Initiative through Grant GBMF4413 to the Rutgers Center for Emergent Materials. Authors thank the DST and Saha Institute of Nuclear Physics, India for facilitating the experiments at the Indian Beamline, Photon Factory, KEK, Japan.

\* [ashna@iiserpune.ac.in](mailto:ashna@iiserpune.ac.in)

<sup>1</sup> I. E. Dzyaloshinskii, JETP **32**, 1259 (1957).

<sup>2</sup> I. E. Dzyaloshinskii, JETP **33**, 807 (1957).

<sup>3</sup> I. Dzyaloshinsky, *Journal of Physics and Chemistry of Solids* **4**, 241 (1958).

<sup>4</sup> T. Moriya, *Phys. Rev.* **120**, 91 (1960).



- <sup>5</sup> U. K. Rossler, A. N. Bogdanov, and C. Pfleiderer, *Nature* **442**, 797 (2006).
- <sup>6</sup> Y. Onose, T. Ideue, H. Katsura, Y. Shiomi, N. Nagaosa, and Y. Tokura, *Science* **329**, 297 (2010).
- <sup>7</sup> M. Z. Hasan and C. L. Kane, *Rev. Mod. Phys.* **82**, 3045 (2010).
- <sup>8</sup> Y. Yamasaki, H. Sagayama, T. Goto, M. Matsuura, K. Hirota, T. Arima, and Y. Tokura, *Phys. Rev. Lett.* **98**, 147204 (2007).
- <sup>9</sup> B. Binz, A. Vishwanath, and V. Aji, *Phys. Rev. Lett.* **96**, 207202 (2006).
- <sup>10</sup> C. L. Kane and E. J. Mele, *Phys. Rev. Lett.* **95**, 226801 (2005).
- <sup>11</sup> J. Sinova and I. Zutic, *Nature Materials* **11**, 368 (2012).
- <sup>12</sup> V. Barthém, C. Colin, H. Mayaffre, M. Julien, and D. Givord, *Nature Communications* **4**, 2892 (2013).
- <sup>13</sup> I. Gross, L. J. Martínez, J.-P. Tetienne, T. Hingant, J.-F. Roch, K. Garcia, R. Soucaille, J. P. Adam, J.-V. Kim, S. Rohart, A. Thiaville, J. Torrejon, M. Hayashi, and V. Jacques, *Phys. Rev. B* **94**, 064413 (2016).
- <sup>14</sup> J. Gayles, F. Freimuth, T. Schena, G. Lani, P. Mavropoulos, R. A. Duine, S. Blügel, J. Sinova, and Y. Mokrousov, *Phys. Rev. Lett.* **115**, 036602 (2015).
- <sup>15</sup> A. B. Romanov, *Soviet Physics JETP* **11**, 786 (1960).
- <sup>16</sup> A. S. Borovik-Romanov, *Zh. Eksp. Teor. Fiz.* **38**, 1088 (1960).
- <sup>17</sup> V. Andratskii and A. S. Borovik-Romanov, *JETP* **687**, 1036 (1966).
- <sup>18</sup> A. S. Borovik-Romanov, *Ferroelectrics* **162**, 153 (1994).
- <sup>19</sup> R. R. Birss, *Symmetry and Magnetism* (New York: North-Holland Pub. Co., 1964).
- <sup>20</sup> D. Halley, N. Najjari, H. Majjad, L. Joly, P. Ohresser, F. Scheurer, C. Ulhaq-Bouillet, S. Berciaud, B. Doudin, and Y. Henry, *Nature Communications* **5**, 3167 (2014).
- <sup>21</sup> J. Sandonis, J. Baruchel, B. Tanner, G. Fillion, V. Kvardakov, and K. Podurets, *Journal of Magnetism and Magnetic Materials* **104**, 350 (1992).
- <sup>22</sup> S. A. J. Kimber and J. P. Attfield, *J. Mater. Chem.* **17**, 4885 (2007).
- <sup>23</sup> T. G. Phillips, R. L. Townsend, and R. L. White, *Phys. Rev. Lett.* **18**, 646 (1967).
- <sup>24</sup> T. G. Phillips, R. L. Townsend, and R. L. White, *Phys. Rev.* **162**, 382 (1967).
- <sup>25</sup> J. Kushauer, W. Kleemann, J. Mattsson, and P. Nordblad, *Phys. Rev. B* **49**, 6346 (1994).
- <sup>26</sup> S. Sahoo and C. Binek, *Philosophical Magazine Letters* **87**, 259 (2007).
- <sup>27</sup> A. Bajpai, R. Klingeler, N. Wizen, A. K. Nigam, S.-W. Cheong, and B. Bchner, *Journal of Physics: Condensed Matter* **22**, 096005 (2010).
- <sup>28</sup> A. Bajpai, Z. Aslam, S. Hampel, R. Klingeler, and N. Grobert, *Carbon* **114**, 291 (2017).
- <sup>29</sup> A. Michels, D. Mettus, D. Honecker, and K. L. Metlov, *Phys. Rev. B* **94**, 054424 (2016).
- <sup>30</sup> S. Mørup and C. Frandsen, *Phys. Rev. Lett.* **92**, 217201 (2004).
- <sup>31</sup> M. J. Benítez, O. Petravic, H. Tüysüz, F. Schüth, and H. Zabel, *Phys. Rev. B* **83**, 134424 (2011).
- <sup>32</sup> M. J. Benitez, O. Petravic, E. L. Salabas, F. Radu, H. Tüysüz, F. Schüth, and H. Zabel, *Phys. Rev. Lett.* **101**, 097206 (2008).
- <sup>33</sup> L. Néel, *Rev. Mod. Phys.* **25**, 58 (1953).
- <sup>34</sup> K. Binder and A. P. Young, *Rev. Mod. Phys.* **58**, 801 (1986).
- <sup>35</sup> J. Mattsson, C. Djurberg, and P. Nordblad, *Phys. Rev. B* **61**, 11274 (2000).
- <sup>36</sup> M. Suzuki, I. S. Suzuki, and M. Matsuura, *Phys. Rev. B* **73**, 184414 (2006).
- <sup>37</sup> M. Lisunova, N. Holland, O. Shchepelina, and V. V. Tsukruk, *Langmuir* **28**, 13345 (2012).
- <sup>38</sup> X. Liu, J. Zhang, S. Wu, D. Yang, P. Liu, H. Zhang, S. Wang, X. Yao, G. Zhu, and H. Zhao, *RSC Adv.* **2**, 6178 (2012).
- <sup>39</sup> X. Liu, H. Wang, C. Su, P. Zhang, and J. Bai, *Journal of Colloid and Interface Science* **351**, 427 (2010).
- <sup>40</sup> In SQUID magnetometers, even in  $H = 0$ , there can be some residual magnetic field arising from the superconducting coil. The magnitude of this residual field can be 5 to 10 Oe and its sign can be arbitrary. Magnetization arising due to this residual field can interfere with the actual remanence. The vanishingly small value of remanence at  $H = 3$  Tesla also sets the base line for any artifacts arising from such residual fields.
- <sup>41</sup> It is also to be noted that for the data on  $\alpha$ -Fe<sub>2</sub>O<sub>3</sub> shown in the inset of Fig.5, the  $H$  during FC cycle is applied when the sample is already in WFM region. This is unlike the case of MnCO<sub>3</sub> and FeCO<sub>3</sub>, when the  $H$  can applied much above the AFM-PM transition temperature, after conclusion of each  $M_{FC}$  and corresponding  $\mu_{FC}$  run. In case of  $\alpha$ -Fe<sub>2</sub>O<sub>3</sub>, it is not practically possible to heat the sample till 950K, after each run.